Non Linear, Two Fluid Magnetohydrodynamic Simulations of Internal Kink Mode in Tokamaks

F.D. HALPERN, H. LÜTJENS, J.-F. LUCIANI

Centre de Physique Théorique, CNRS, École Polytechnique, 91120 Palaiseau, France

e-mail: fhalpern@cpht.polytechnique.fr

Abstract

The dynamics of the internal kink mode, which drives sawtooth oscillations in tokamaks, are studied in numerical simulations carried out using the XTOR-2F code. The work is carried out using a three dimensional, non-linear magnetohydrodynamic model that includes resistivity, anisotropic transport, and ion and electron diamagnetic flows. It is found that a threshold of diamagnetic stabilization differentiates an oscillation regime characterized by oscillations with slow crash times from an oscillating regime characterized by sawtooth-like dynamics and short crash times. The simulation results indicate that diamagnetic effects may be sufficient to drive sustained kink oscillations with sawtooth-like behavior in Ohmic tokamak plasmas.

1. Introduction

Sawtooth oscillations are characterized by a magnetic reconnection event with helicity $q = m/n = 1/1$ that periodically redistributes heat, current, and particles in the plasma core of magnetically confined devices [1]. Increased understanding of sawtooth dynamics is necessary for successful ITER operation. It is believed that sawtooth crashes in tokamak plasmas can "seed" neoclassical tearing modes, and that they can trigger kinetic instabilities that result in loss of confinement for fast ions (see, for example [2, 3, 4]).

Some aspects of sawtooth physics are still not very well understood. In ideal magnetohydrodynamics (MHD), an unstable kink mode leads to non-linear saturation, i.e. it results in a three dimensional equilibrium with helicity $m/n = 1/1$. Non-decaying kink oscillations can be recovered in resistive MHD at low poloidal beta ($\beta_p = 2\mu_0 p/B_\theta^2$). However, resistive MHD kink oscillations exhibit crash times that are several orders of magnitude too slow compared to the crash times observed in large tokamaks. A priori, the large instability growth rates required for a short crash time (in the ideal MHD time scale) seem at odds with the slow growth rate (in the resistive time scale) required to sustain sawtooth cycling characterized by quiescent ramps. Several models for the sawtooth crash explaining the acceleration of the growth rate during the late stage of the sawtooth ramp have been proposed [5, 6, 7, 8, 9].

The bifurcation between a pressure-driven saturating kink mode and an oscillating kink mode was the subject of a recent study [10]. It was found that the thresholds for sustained kink oscillations depended on the ratio of the resistive diffusion time $\tau_\eta = \mu_0 a^2/\eta$ to the perpendicular energy diffusion time $\tau_{\chi_\perp} = a^2/\chi_\perp$, the poloidal beta, and the diamagnetic stabilization (which scales like the inverse of the ion cyclotron frequency). However, even in kink mode simulations carried out including diamagnetic flows, the sustained kink oscillations resulted in pressure oscillations more or less corresponding to Kadomtsev's scaling for the sawtooth crash time ($\tau_{crash} \sim S^{1/2}$, $S \sim 1/\eta$ is the Lundquist

number) [11]. In only one simulation in reference [10] it was found that the collapse of the pressure ($\tau_{collapse} \approx 600\tau_a$) was short respect to the ramp time ($\tau_{ramp} \approx 25000\tau_a$).

In the present work, magnetohydrodynamic (MHD) numerical simulations including resistivity, transport, and diamagnetic flows are used to study the transition between a regime of sustained kink oscillations with Kadomtsev like crashes and a regime of sustained kink oscillations with sawtooth-like behavior and fast crashes. In particular, it will be shown that the transition between the two regimes depends on a ratio of resistivity respect to the diamagnetic stabilization of the internal kink mode growth rate. It is hypothesized that in high temperature plasmas with Lundquist number $S \sim 10^8$ the ramp of the resistive internal kink is almost always strongly modified by the diamagnetic stabilization. In most Ohmic plasmas with circular cross section, this phenomenon would lead to sustained kink oscillations with fast crashes.

In the next section, the physical model used to carry out the study is described briefly. Then, the oscillation regimes are described in section 3. A discussion regarding the thresholds for sustained kink oscillations is found in section 4. The conclusions of the study are presented in section 5.

2. Physical model

The physical model used to study the dynamics of the internal kink mode is briefly summarized here. The simulations are carried out with the XTOR-2F code, which is described in detail in reference [12]. The physical model is fully toroidal and non-linear; and it includes anisotropic thermal transport, resistivity, viscosity, and diamagnetic drifts. The equation system, which is a subset of the Braginskii two-fluid system [13], reads

$$\rho\partial_t\mathbf{v} = -\rho\left(\mathbf{v}\cdot\nabla\right)\mathbf{v} - \rho\left(\mathbf{v_i^*}\cdot\nabla\right)\mathbf{v}_\perp + \mathbf{J}\times\mathbf{B} - \nabla\mathbf{p} + \nu\nabla^{\mathbf{2}}\mathbf{v}, \quad (1)$$

$$\partial_t\mathbf{B} = \nabla\times\left(\mathbf{v}\times\mathbf{B}\right) + \alpha\nabla\times\nabla_\parallel p_e/\rho - \nabla\times\eta\mathbf{J}, \quad (2)$$

$$\partial_t p = \Gamma p\nabla\cdot\mathbf{v} - \mathbf{v}\cdot\nabla p - \alpha\Gamma\frac{p}{\rho}\nabla p_i\cdot\nabla\times\mathbf{B}/B^2 + \nabla\cdot\chi_\perp\nabla_\perp p + \nabla\cdot\chi_\parallel\nabla_\parallel p - \Theta, \quad (3)$$

$$\partial_t\rho = -\rho\nabla\cdot\mathbf{v} - \mathbf{v}\cdot\nabla\rho - \alpha\nabla p_i\cdot\nabla\times\mathbf{B}/B^2 + \nabla\cdot D_\perp\nabla\rho - \Sigma. \quad (4)$$

The diamagnetic flow terms are scaled using the constant $\alpha = (\omega_{ci}\tau_a)^{-1}$ ($\omega_{ci} = eB_u/m_i$ and $\tau_A = (\mu_0\rho_0)^{1/2}\,a/B_u$ is the Alfvén time, $B_u = aB_0/R_0$ is the unit magnetic field), while $\mathbf{v}_i^* = \alpha\mathbf{B}\times\nabla p_i/(\rho B^2)$ is the ion diamagnetic velocity. The perpendicular diffusive source terms in equations 3 and 4, $\Theta = \nabla\cdot\chi_\perp\nabla_\perp p_{t=0}$ and $\Sigma = \nabla\cdot D_\perp\nabla\rho_{t=0}$, restore the pressure and density profiles within their characteristic diffusion times. In the above equations, $\eta = \eta_0(p/p_0)^{-3/2}$ is the resistivity, $\chi_\perp = \chi_{\perp 0}(p/p_0)^{-3/2}$ is the thermal diffusivity, $D = \chi_\perp/10$ is the particle diffusivity, $\nu = 5.0\times10^{-6}$ is the viscosity, and $\Gamma = 5/3$ is the ratio of specific heats. In the simulations, these quantities are all constant in time. Equal ion and electron pressure are assumed, $p_e = p_i = p/2$. Resistive MHD plus transport ($\eta\chi$MHD) are recovered by setting $\alpha = 0$.

3. Simulation results

In this section, the results of the non-linear simulations are described. We are interested in studying the non-linear steady state of the oscillations, that is, the simulations

must be evolved until the amplitude and frequency of the kink oscillations becomes constant, or until the kink mode saturates. Non-linear kink mode simulations are carried out including the toroidal harmonics $n = 0, 1, 2, 3$. For $n = 1, 2, 3$, the harmonics retained have $n - 4 \leq m \leq n + 7$, *i.e.* harmonics with $q \neq 1$ are included. The $n = 0$ mode, for which 8 poloidal modes are retained, initially corresponds to the equilibrium fields. The starting equilibrium is computed using the CHEASE code [14]. The equilibrium boundary is circular, with aspect ratio $R/a = 2.7$. The pressure and magnetic q profiles used for the study are shown in figure 1. The equilibrium has a parabolic q profile with $q_0 = 0.77$, $q_{edge} = 5.4$, $\hat{s}_{q=1} = 0.4$ ($\hat{s} = (r/q)(dq/dr)$). The radial profile of poloidal beta, $\beta_p = 2\mu_0 p/B_\theta^2$, is almost flat. The equilibrium used in the simulations has $\beta_p \approx 0.22$, which is about 2/3 of threshold for the ideal MHD kink ($\beta_p = 0.33$). The ideal instability threshold was determined in XTOR-2F simulations of the quasi-linear growth phase with $n = 0$ and $n = 1$ only.

The relevant time scales of the plasma dynamics are given by the resistive diffusion time $\tau_\eta = 1/\eta = S$, which affects the growth rate of the internal kink and the relaxation of the q profile after each crash; and the characteristic energy diffusion time $\tau_{\chi_\perp} = 1/\chi_\perp$, which acts through the source term in equation 3. (The characteristic times are given in internal units, $a = 1$, $\mu_0 = 1$). Simulations are carried out using $\tau_\eta/\tau_{\chi_\perp} = \chi_\perp/\eta = 30$, while in tokamak experiments $\tau_\eta/\tau_{\chi_\perp} \approx 100$.

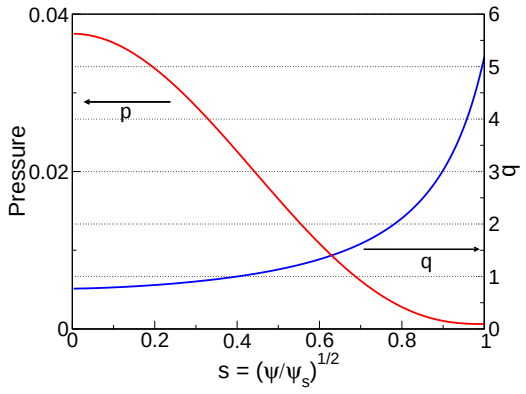

Figure 1: *Initial equilibrium pressure and q profiles.*

An additional time scale in the kink dynamics is introduced by the diamagnetic stabilization. In the resistivity dominated regime with diamagnetic stabilization, the linear growth rate of the resistive kink can be expressed in the form $\gamma \sim S^{-1/3} - \alpha$ [15]. Thus, in order to rescale the diamagnetic stabilization as the resistivity is varied, it is expected that the quantity $S^{-1/3}/\alpha$ should be kept constant. For instance, in the JET tokamak, using $R_0 = 3.1$m, $B_0 = 2.7$T, $n_0 = 2.0 \times 10^{19}$m^{-3}, $T_e = 2$keV (typical of Ohmic plasmas), we obtain $\alpha \approx 0.08$ and $S \approx 2 \times 10^8$. Keeping $S^{-1/3}/\alpha$ constant, but decreasing the Lundquist number to $S = 10^7$ we find $\alpha \approx 0.24$. In the present paper, $S = 10^6 - 10^7$ and $\alpha = 0 - 0.2$. The influence of this additional time scale will be demonstrated in the simulation results.

Three different kink oscillation regimes are recovered in the simulations: a quasi-helicoidal equilibrium characterized by a $m/n = 1/1$ saturated kink; an oscillating kink with non-decaying oscillations with slow, resistivity-driven crashes; and an oscillating kink with non-decaying oscillations and fast crashes. Below, we describe the dynamics of the oscillating kinks with fast crashes, and compare and contrast with the other regimes as required.

Figure 2 shows the pressure evolution of a simulation carried out with $\beta_p = 0.22$, $S = 2/3 \times 10^7$, and $\alpha = 0.15$. Following a long quiescent ramp, a slowly growing precursor appears, causing the central pressure to slowly spiral out towards the $q = 1$ surface. The mode appears to quasi-saturate. Then, there is a change in the time scale the crash is taking place, with the kinetic energy of the modes increasing by a factor of three in less

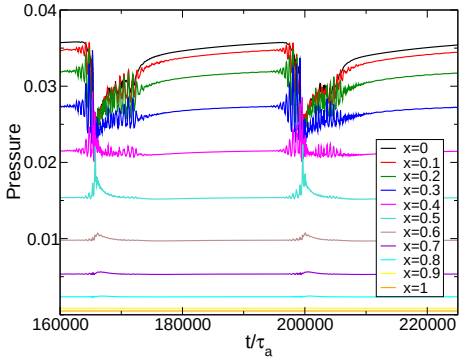

Figure 2: *Pressure vs. time in simulation with accelerated kink crashes.*

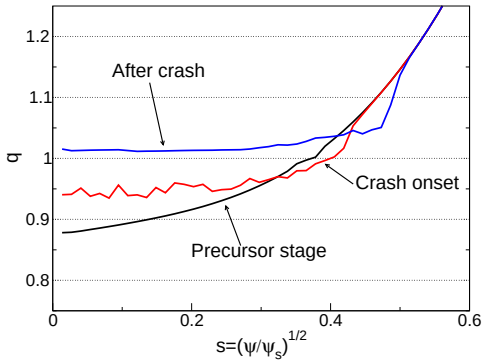

Figure 3: *Evolution of the q profile during the kink cycle.*

than $500\tau_a$. Following the crash, there is a long-lived post-cursor mode of mixed helicity, which drives a secondary pressure crash. The evolution of the q profile is shown in figure 3. The magnetic q at the axis, q_0, is about 0.9 at the beginning of the precursor stage. The precursor flats out the q profile around the $q = 1$ magnetic surface as it grows, but $q_0 < 0$ before the crash. Following the crash, $q > 1$ inside the mixing radius of about 45%. As the precursor damps away, q_0 starts to drop and the cycle restarts.

Poloidal cross sections of the magnetic field up to $s = (\psi/\psi_s)^{1/2} \approx 0.5$ are displayed for this case in figures 4-7 in order to illustrate the different stages of the oscillation. Figure 4 shows the $m/n = 1/1$ precursor island. As this precursor grows, it displaces the pressure core toward the $q = 1$ surface, and a thin plasma ribbon between the two ends of the island forms. Figure 5 shows the precursor island at the end of the precursor stage. During the crash phase, as shown in figure 6, the reconnection process accelerates and an X-point forms [7, 8, 16]. Following the crash, the inner 30% of the plasma radius is occupied by remains of the precursor chain, with mixed $n = 1, 2, 3$ helicity. In the present case, the postcursor islands are long-lived, driving a secondary reconnection event that takes place in a slower time scale than the principal crash. After some time, the postcursor modes damp away, leading to a quiescent ramp with a slow pressure core recovery.

In order to illustrate the difference between the oscillations with accelerated crashes and the oscillations with resistive crashes, the central pressure as a function of time is shown for several oscillating cases. The pressure observed in each simulation is shown within a short time window around t_0, which indicates the time of lowest central pressure during a kink cycle. Thus, it is possible to compare the pressure evolution of different cases around the crash time. Figure 8 shows the central pressure as a function of time for four different XTOR-2F simulations carried out at different resistivity, and using both diamagnetic drifts. The Lundquist number is varied between $S = 10^6$ and $S = 10^7$. The rate of change of the pressure as a function of time is highest at high resistivity. It is noted that it appears that both the pressure rise and fall rates are higher with higher resistivity. The evolution of the central pressure during the crash denotes Kadomtsev-like behaviour, i.e., the duration of the pressure crash scales like the resistivity. The recovery of the pressure core also takes place in the resistive time scale. In essence, the rise and decay times of the pressure indicate behaviour similar to kink oscillations in $\eta\chi$MHD, with poorly separated time scales denoted by similar ramp and crash times.

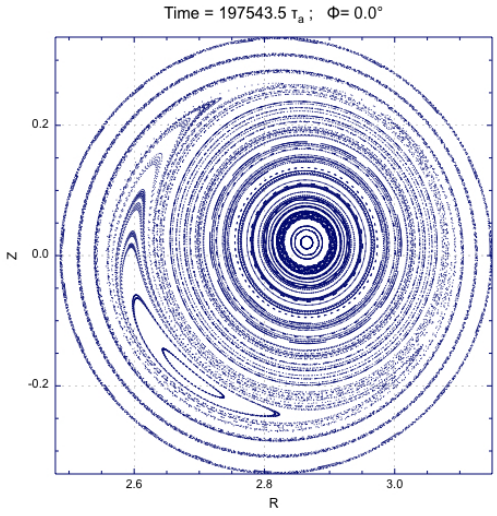

Figure 4: *Magnetic field cross section during precursor stage.*

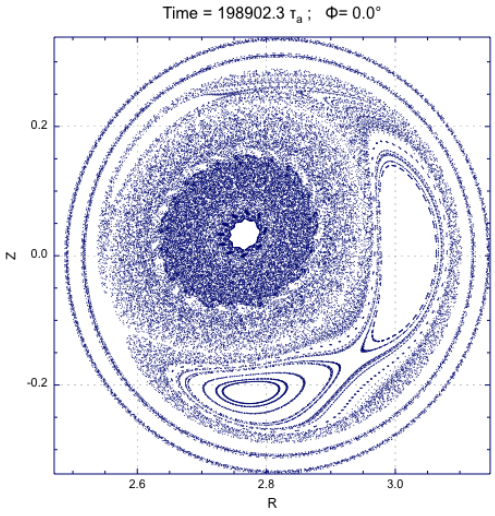

Figure 5: *Magnetic field cross section at the crash onset.*

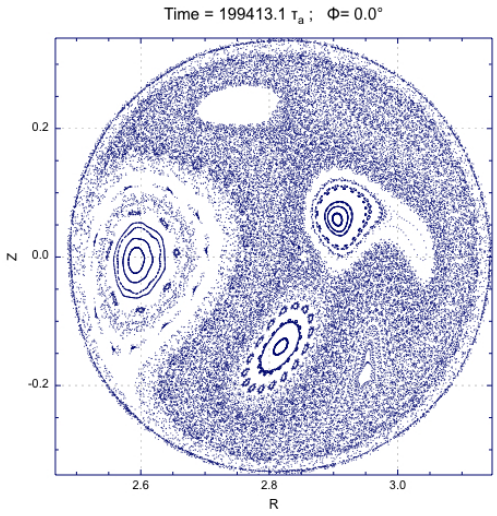

Figure 6: *Magnetic field cross section during the crash.*

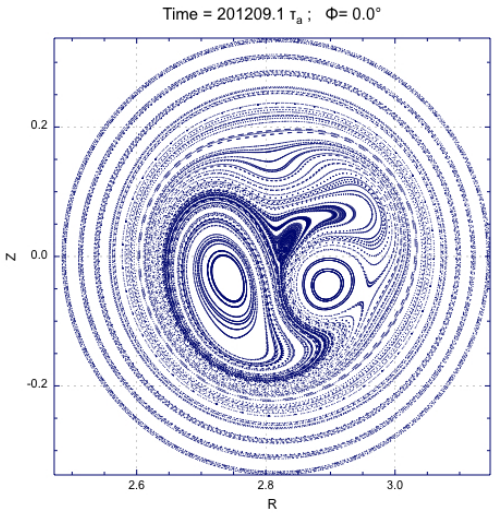

Figure 7: *Magnetic field cross section during postcursor stage.*

Figure 9 shows the central pressure evolution obtained in simulations carried out with α, $S = 1/3 \times 10^6 - 10^7$ and $\alpha = 0.075 - 0.15$, i.e. the resistivity is varied by a factor of three and the strength of the diamagnetic flow is varied by a factor of two. The fast crash regime is inaccessible at $S = 10^6$ because of numerical limitations (the α required to reach the critical diamagnetic stabilization threshold is too high). Respect to figure 8, the crashes take place in a much shorter time frame, with better separated time scales. The pressure collapse time is similar for all resistivities, varying between $300\tau_a$ and $600\tau_a$. Using the experimental figures at the beginning of section 3, this is equivalent to about $100 - 200\mu$s. When the periods and amplitudes of the pressure oscillations obtained in the simulations are compared, several trends arise. The amplitude of the pressure

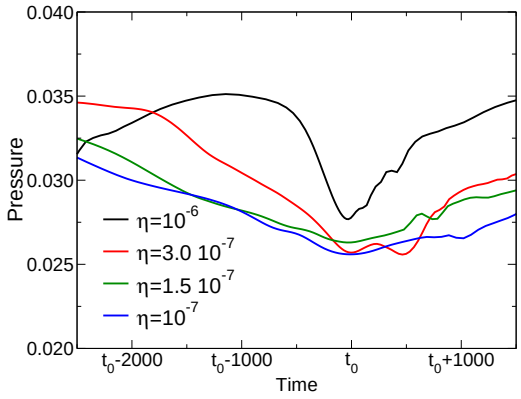

Figure 8: *Central pressure vs. time is shown for XTOR-2F simulations in the resistive kink regime.*

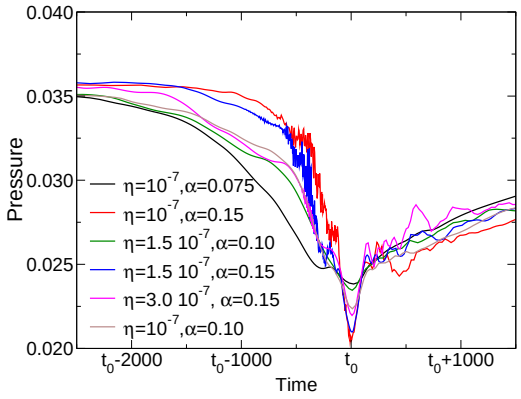

Figure 9: *Central pressure vs. time is shown for XTOR-2F simulations in the diamagnetic kink regime.*

oscillations obtained with the fast crashes is between 30% and 45%; while the amplitude of the pressure oscillations obtained with the resistive crashes is generally in the order of 25%. The oscillation periods increase with increasing S or α. The dependence of the oscillation thresholds respect to the resistivity and the diamagnetic flows are discussed in the section below.

4. Threshold for sustained oscillations with fast crashes

In this section, the plasma conditions required for transition between the different oscillation regimes are discussed. The relevant parameter space for each oscillation regimes are obtained by carrying out simulations including both diamagnetic drifts at $\beta_p = 0.22$, $\tau_{\chi\perp} = 30$, $D_\perp = \chi_\perp/10$, and $\chi_\parallel/\chi_\perp \approx 10^7$. Different regimes are observed in the simulations by varying $\alpha = 0 - 0.2$ and $S = 10^6 - 10^7$.

The pattern of oscillations using the diamagnetic model, as a function of $S = 1/\eta$ and α, is shown in figure 10. The circles represent sustained oscillations with Kadomtsev-like resistive crashes, the triangles represent sustained oscillations with accelerated crashes, and the squares represent saturated kinks. Saturated kinks, which are characterized by a helicoidal equilibrium with a saturated $m/n = 1/1$ island, are obtained in $\eta\chi$MHD ($\alpha = 0$) and at low α. As the diamagnetic stabilization is increased, the saturated kink is stabilized and sustained oscillations are observed. Further increasing α yields a second transition to a regime where the sustained oscillations are characterized by quiescent ramps followed by a precursor stage and an accelerated crash. This change in the characterization of the internal kink ramp is observed as a sharp transition as α is increased.

The cycle dynamics recovered can be described as a competition between the relaxation of the q profile after each crash, the sources that rebuild the pressure core, and the diamagnetic stabilization. The diamagnetic flow stabilizes first a pressure driven, low shear instability that results in a saturated kink with helicity $m/n = 1/1$. This effect gives rise to sustained resistive oscillations in which the dynamics are similar to $\eta\chi$MHD. If the resistive kink is strongly stabilized by the diamagnetic flow, a second transition occurs,

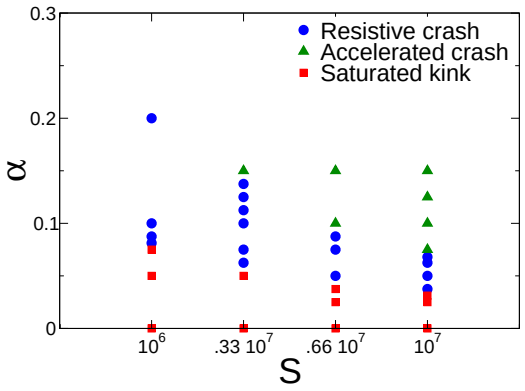

Figure 10: *Oscillating regimes found as a function of* $\alpha = (\omega_{ci}\tau_a)^{-1}$ *and* $S = 1/\eta$.

with the dynamics of the kink oscillations then strongly modified by diamagnetic effects. An exponential fit to the saturation-oscillation threshold yield $\alpha \propto S^{-0.33}$, which can be readily identified as the effect of quasi-linear growth rate stabilization due to diamagnetic flows. The transition from oscillating kinks to oscillating kinks with fast crashes gives the fit $\alpha \propto S^{-0.6}$.

Note that, while it is not possible to carry out simulations at realistic Lundquist numbers, the results of the parameter scan carried out indicates that, in high temperature plasmas ($S \sim 10^8$), diamagnetic effects alone may be sufficient to trigger sawtooth crashes in tokamaks. For instance, accelerated crashes are recovered with $\alpha = 0.075$ at $S = 10^7$, while in $\alpha \approx 0.08$ in Ohmic discharges. Furthermore, the Kadomtsev-like crashes may be inaccessible at experimental resistivities in large tokamaks. This phenomenon is due to the different stabilization thresholds, i.e. it is easier to reach the stabilization threshold at higher temperature because of the $S^{-1/3}$ vs. $S^{-0.6}$ dependence.

5. Summary and conclusions

In $\eta\chi$MHD with diamagnetic flows (equations 1-4), the ramp dynamics of the internal kink can be characterized using the quantities $\tau_\eta/\tau_{\chi_\perp} = \chi_\perp/\eta$, β_p, and $\alpha = (\omega_{ci}\tau_a)^{-1}$. The present paper attempts to quantify the scaling of some plasma conditions necessary to trigger an acceleration of the reconnection event during a kink crash. A parameter scan in S and α revealed a pattern of saturated kinks, oscillating kinks with resistive crashes, and oscillating kinks with accelerated crashes. The transition from saturated kink to oscillating kink was found to occur when a constant value of $S^{-1/3}/\alpha$ is exceeded. On the other hand, the transition from slow to fast crashing kinks occurs at constant $S^{-0.6}/\alpha$.

The oscillating kinks with slow crashes are characterized by Kadomtsev-like resistive reconnection. The crash dynamics in these cases are several orders of magnitude too slow to explain the fast crash times observed in experiments. Even with diamagnetic flows, these kink oscillations are very similar to $\eta\chi$MHD kink oscillations, except for the presence of rotating island chains that remain around $q = 1$ following each crash.

On the contrary, the dynamics of the kink oscillations with accelerated crashes are in some ways similar to the sawtooth oscillations observed in tokamaks. The crash occurs in two phases, which involve a slowly growing precursor and a phase of accelerated

reconnection triggered by diamagnetic effects. The pressure collapse time is much shorter than the ramp time, and the crash time is not very sensitive to the resistivity. At constant η, the crash time is shortened with increasing α. It is noted that the MHD model for the reconnection used in the simulations is not complete, and that including electron inertia and polarization drift terms may shorten the crash time or alter the scaling of the threshold for accelerated reconnection.

Using the present model, the sawtooth crash can be interpreted as a transition from a slowly growing resistive mode to a rapidly growing mode driven by the loss of the electron diamagnetic drift on the reconnection layer, as proposed in [7, 8]. It is observed in the simulations that the parameter window for the resistive MHD-like oscillations decreases as the resistivity is decreased. Consequently, in a two-fluid model the sawtooth ramp at experimental parameters would consist of a quiescent ramp followed by a crash taking place in the 100μs time scale, which is consistent with experimental observations.

This work was carried out within the framework of the European Fusion Development Agreement and the French Research Federation for Fusion Studies (FR-FCM). It is supported by the European Communities under the contract of Association between EURATOM and CEA. The views and opinions expressed herein do not necessarily reflect those of the European Commission.

[1] HASTIE, R. J., Astrophysics and Space Science **256** (1997) 177.

[2] SAUTER, O., et al., Phys. Rev. Letters **88** (2002).

[3] HENDER, T., WESLEY, J., BIALEK, J., et al., Nucl. Fusion **47** (2007) S128.

[4] FASOLI, A., GORMENZANO, C., BERK, H., et al., Nucl. Fusion **47** (2007) S264.

[5] WESSON, J. A., Plasma Phys. Control. Fusion **28** (1986).

[6] AYDEMIR, A. Y., Phys. Rev. Letters **59** (1987) 649.

[7] ZAKHAROV, L., ROGERS, B., and MIGLIUOLO, S., Phys. Fluids B **5** (1993) 2498.

[8] WANG, X. and BHATTACHARJEE, A., Phys. Rev. Letters **70** (1993) 1627.

[9] BISKAMP, D. and DRAKE, J. F., Phys. Rev. Letters **73** (1994).

[10] HALPERN, F. D., LEBLOND, D., LÜTJENS, H., and LUCIANI, J.-F., submitted to Plasma Phys. Control. Fusion(2010).

[11] KADOMTSEV, B. B., Sov. J. Plasma Physics **1** (1975) 389.

[12] LÜTJENS, H. and LUCIANI, J.-F., J. Comput. Phys **229** (2010) 8130.

[13] BRAGNISKII, S. I., Transport processes in a plasma, volume 1 of Reviews of plasma physics, Consultants Bureau, New York, 1965.

[14] LÜTJENS, H., BONDESON, A., and SAUTER, O., Comp. Phys. Communication **97** (1996) 219.

[15] ARA, G., BASU, B., COPPI, B., et al., Annals of Physics **112** (1978) 443.

[16] ROGERS, B. and ZAKHAROV, L., Phys. Plasmas **3** (1996) 2411.